Supplement of Atmos. Chem. Phys., 25, 12615–12628, 2025
https://doi.org/10.5194/acp-25-12615-2025-supplement

Atmospheric Chemistry and Physics
Open Access

Supplement of

Acid-catalyzed hydrolysis kinetics of organic hydroperoxides: computational strategy and structure–activity relationship

Qiaojing Zhao et al.

Correspondence to: Rujing Yin (yinrj@dlut.edu.cn) and Hong-Bin Xie (hbxie@dlut.edu.cn)

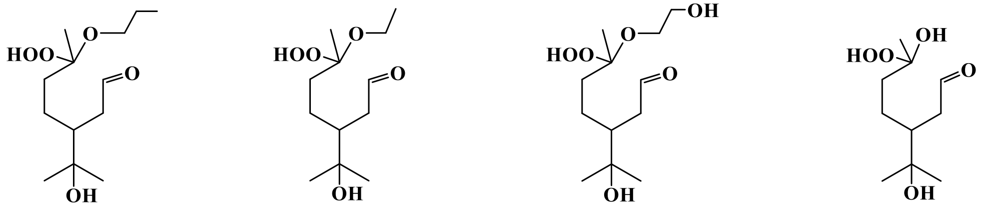

(a) C_{13} α-AH
$C_{13}H_{26}O_5$, MW = 262

(b) C_{12} α-AH$_{(1)}$
$C_{12}H_{24}O_5$, MW = 248

(c) C_{12} α-AH$_{(2)}$
$C_{12}H_{24}O_6$, MW = 264

(d) C_{10} α-HH
$C_{10}H_{20}O_5$, MW = 220

Figure S1. Structures of selected four ROOHs for screening protonated water cluster model (Qiu et al., 2020; Enami, 2022; Hu et al., 2022). Structure **(a)** is C_{13} α-AH derived via α-terpineol derived CIs and 1-propanol, **(b)** is C_{12} α-AH$_{(1)}$ derived via α-terpineol derived CIs and ethanol, **(c)** is C_{12} α-AH$_{(2)}$ derived via α-terpineol derived CIs and ethylene glycol, and **(d)** is C_{10} α-HH derived via α-terpineol derived CIs and water. The corresponding chemical formulas and molecular weights (MW, amu) are labelled.

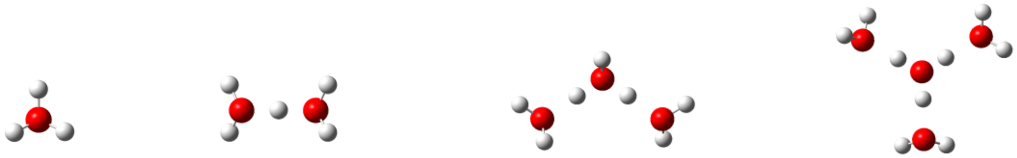

(a) $H^+(H_2O)_1$

(b) $H^+(H_2O)_2$

(c) $H^+(H_2O)_3$

(d) $H^+(H_2O)_4$

Figure S2. Minimum-energy structures of protonated water cluster **(a)** $H^+(H_2O)_1$, **(b)** $H^+(H_2O)_2$, **(c)** $H^+(H_2O)_3$, **(d)** $H^+(H_2O)_4$. The atoms in red and white represent oxygen and hydrogen atoms, respectively.

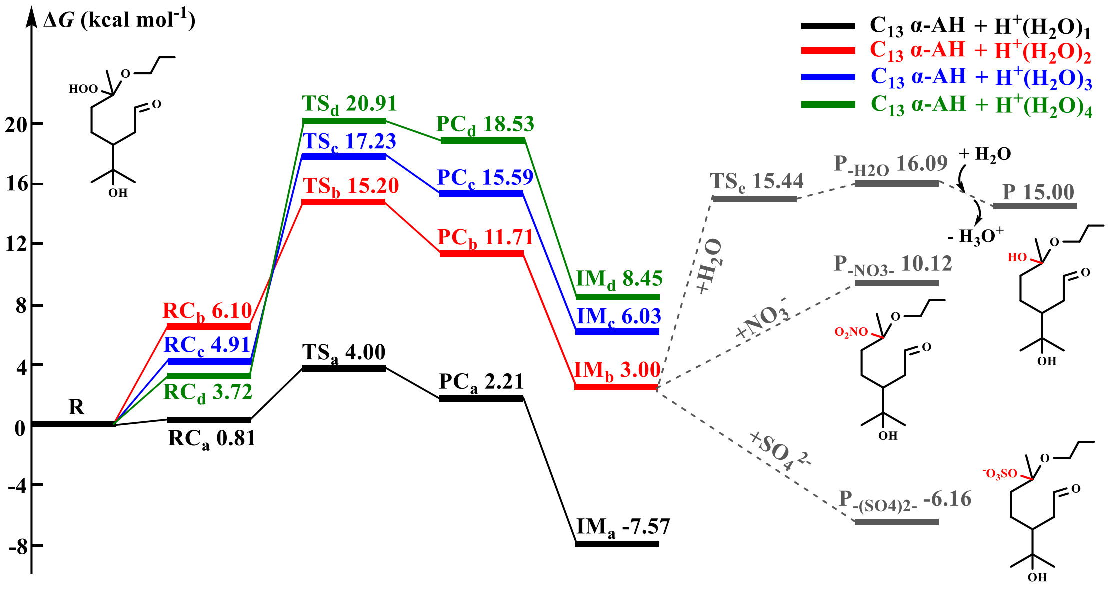

Figure S3. Calculated free-energy surfaces for acid-catalyzed hydrolysis of C_{13} α-AH in four different cases at the SMD/M06-2X/6-311++G(3df,2pd)//M06-2X/6-31+G(d,p) level. The free energies of ROOH and $H^+(H_2O)_n$ (n = 1, 2, 3, 4) are set to zero (reference state, R). RC, TS_x (x = a, b, c, d, e), PC, IM and P represent pre-reactive complexes, transition states, post-reactive complexes, intermediates and products, respectively.

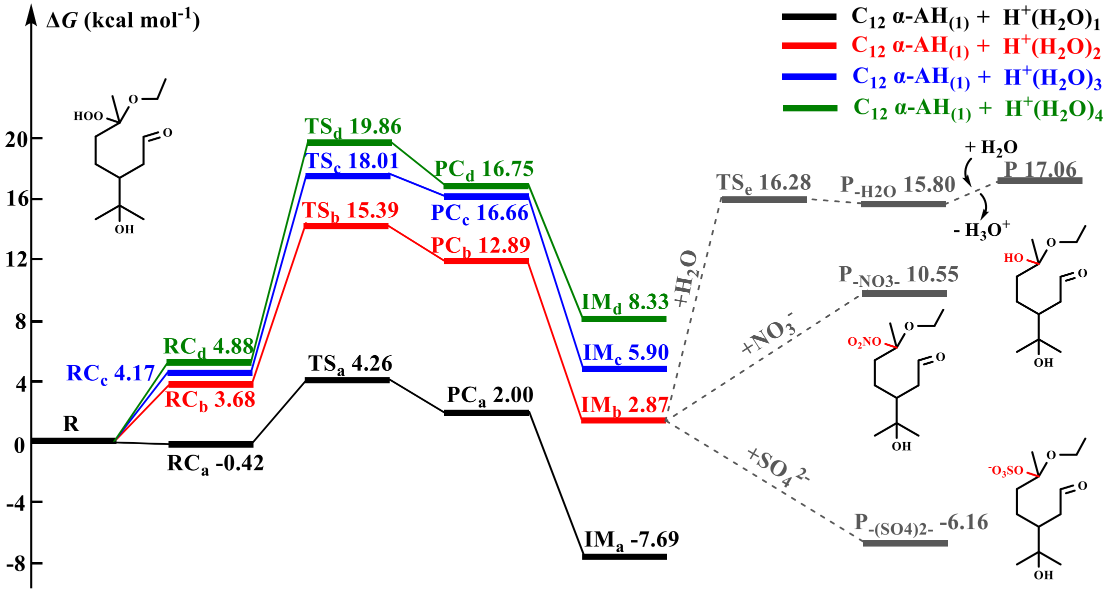

Figure S4. Calculated free-energy surfaces for acid-catalyzed hydrolysis of C_{12} α-$AH_{(1)}$ in four different cases at the SMD/M06-2X/6-311++G(3df,2pd)//M06-2X/6-31+G(d,p) level. The free energies of ROOH and $H^+(H_2O)_n$ (n = 1, 2, 3, 4) are set to zero (reference state, R). RC, TS_x (x = a, b, c, d, e), PC, IM and P represent pre-reactive complexes, transition states, post-reactive complexes, intermediates and products, respectively.

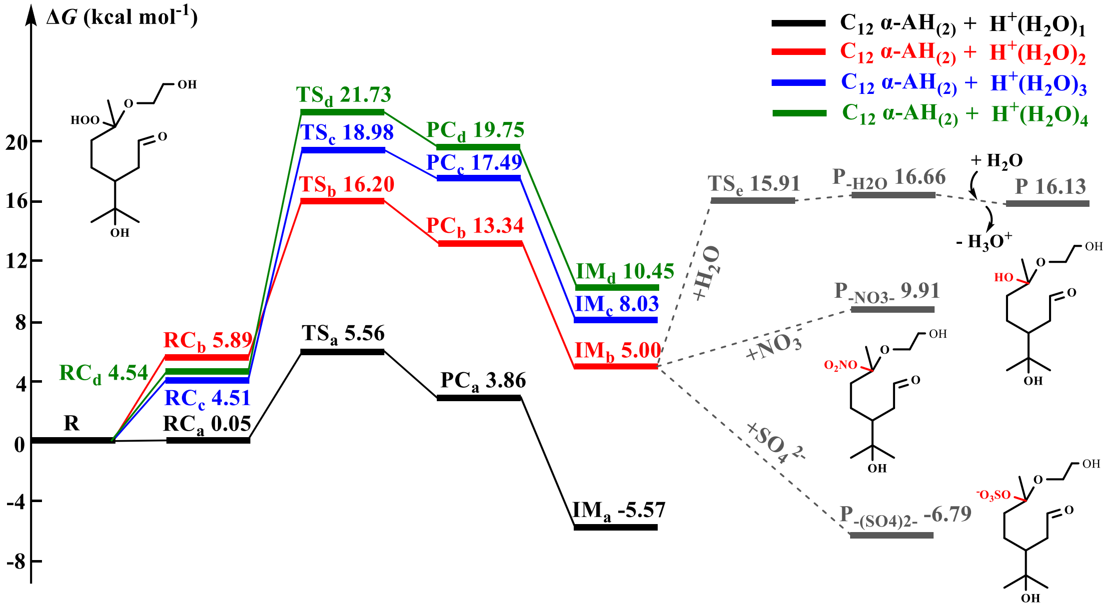

Figure S5. Calculated free-energy surfaces for acid-catalyzed hydrolysis of C_{12} α-$AH_{(2)}$ in four different cases at the SMD/M06-2X/6-311++G(3df,2pd)//M06-2X/6-31+G(d,p) level. The free energies of ROOH and $H^+(H_2O)_n$ ($n = 1, 2, 3, 4$) are set to zero (reference state, R). RC, TS_x (x = a, b, c, d, e), PC, IM and P represent pre-reactive complexes, transition states, post-reactive complexes, intermediates and products, respectively.

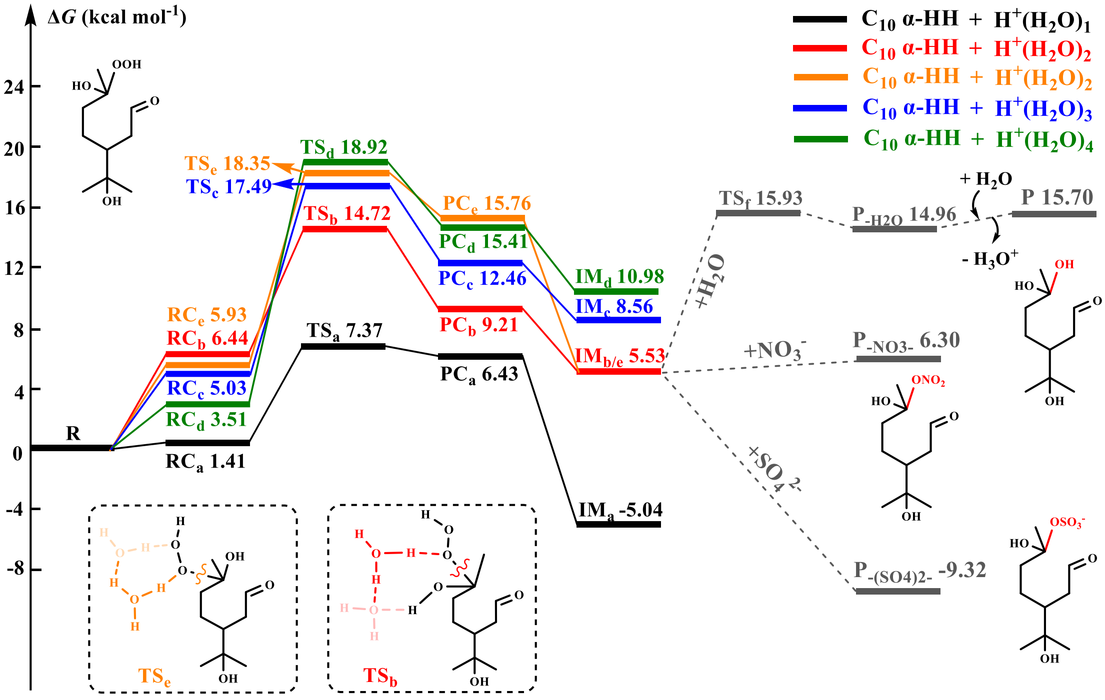

Figure S6. Calculated free-energy surfaces for acid-catalyzed hydrolysis of C_{10} α-HH in four different cases at the SMD/M06-2X/6-311++G(3df,2pd)//M06-2X/6-31+G(d,p) level. The free energies of ROOH and $H^{+}(H_2O)_n$ (n = 1, 2, 3, 4) are set to zero (reference state, R). RC, TS_x (x = a, b, c, d, e, f), PC, IM and P represent pre-reactive complexes, transition states, post-reactive complexes, intermediates and products, respectively.

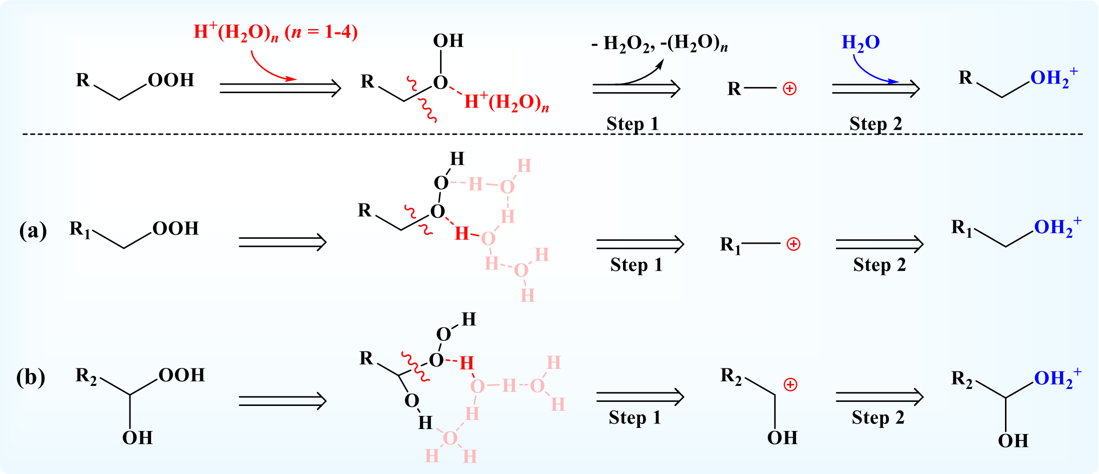

Figure S7. Two-step acid-catalyzed hydrolysis pathway of four ROOHs for screening protonated water cluster model. The reaction pathways **(a)** for C_{13} α-AH, C_{12} α-$AH_{(1)}$, and C_{12} α-$AH_{(2)}$, and **(b)** for C_{10} α-HH.

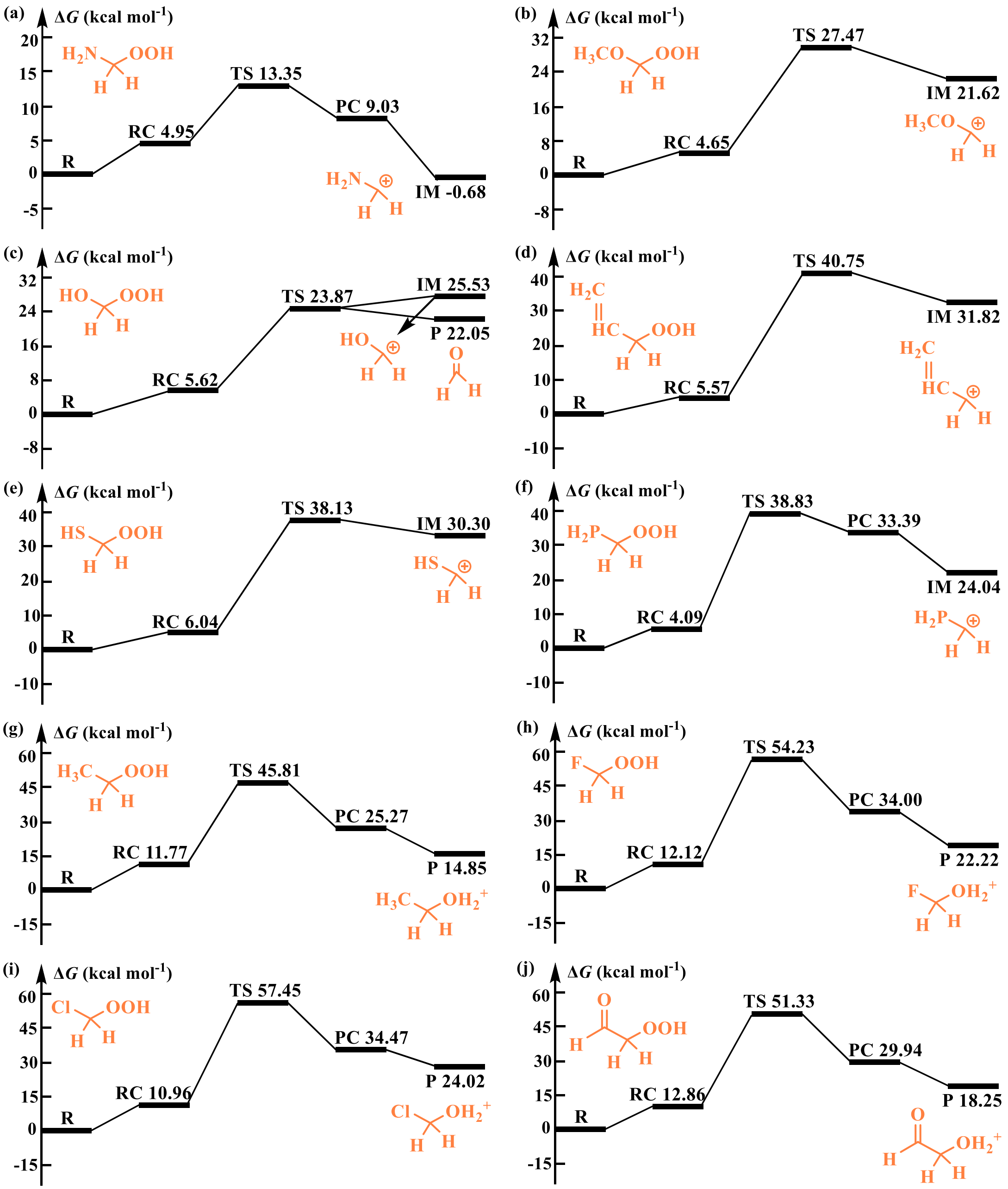

Figure S8. Calculated free-energy surfaces for acid-catalyzed hydrolysis of CH_3CH_2OOH and $CH_2(X)OOH$ (X = NH_2, OCH_3, OH, $CH{=}CH_2$, SH, PH_2, F, Cl and CHO) at the SMD/M06-2X/6-311++G(3df,2pd)//M06-2X/6-31+G(d,p) level. The free energies of ROOH and $H^+(H_2O)_2$ are set to zero (reference state, R). RC, TS, PC, IM and P represent pre-reactive complexes, transition states, post-reactive complexes, intermediates and products, respectively.

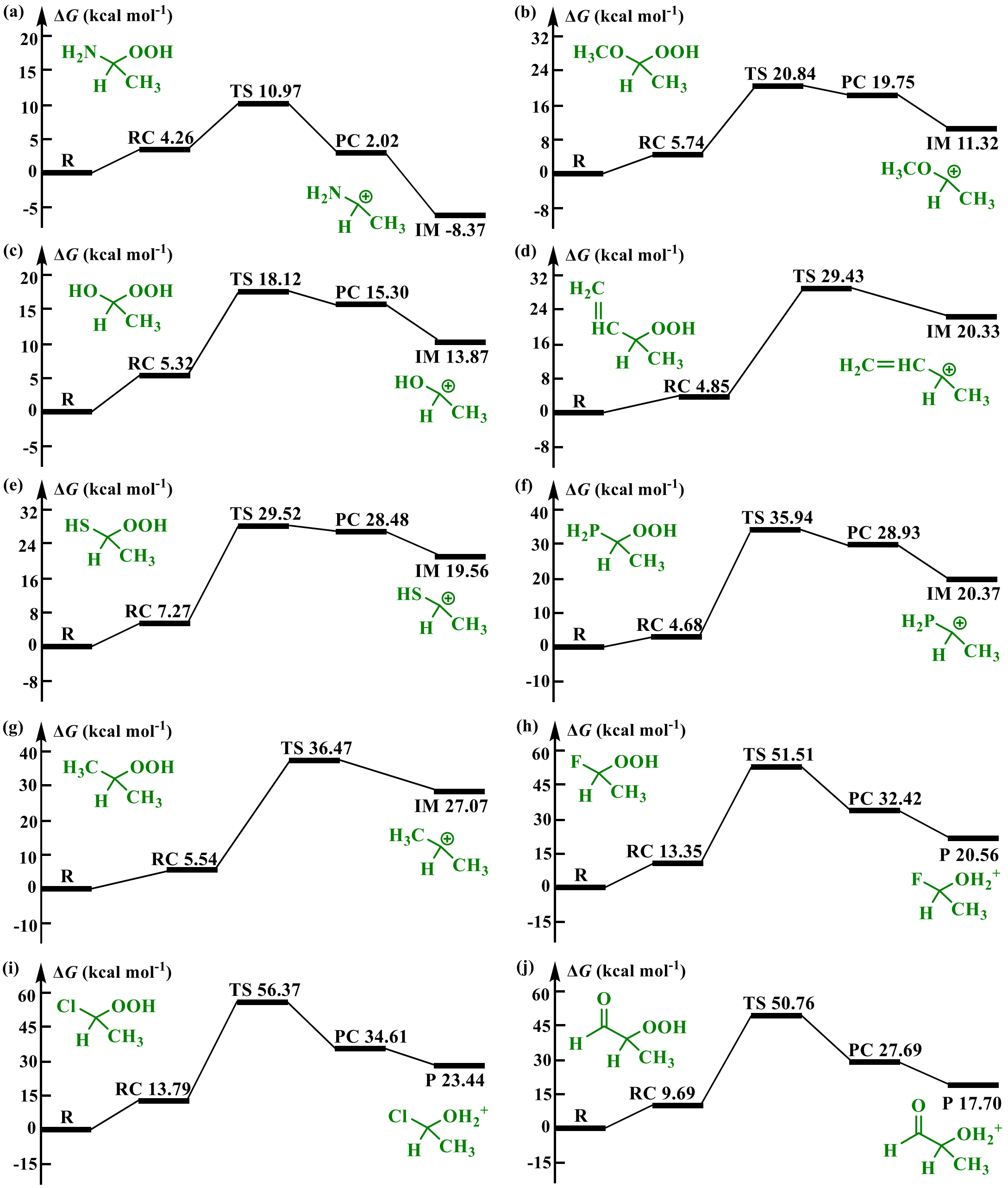

Figure S9. Calculated free-energy surfaces for acid-catalyzed hydrolysis of $CH(CH_3)_2OOH$ and $CH(CH_3)(X)OOH$ ($X = NH_2$, OCH_3, OH, $CH{=}CH_2$, SH, PH_2, F, Cl and CHO) at the SMD/M06-2X/6-311++G(3df,2pd)//M06-2X/6-31+G(d,p) level. The free energies of ROOH and $H^+(H_2O)_2$ are set to zero (reference state, R). RC, TS, PC, IM and P represent pre-reactive complexes, transition states, post-reactive complexes, intermediates and products, respectively.

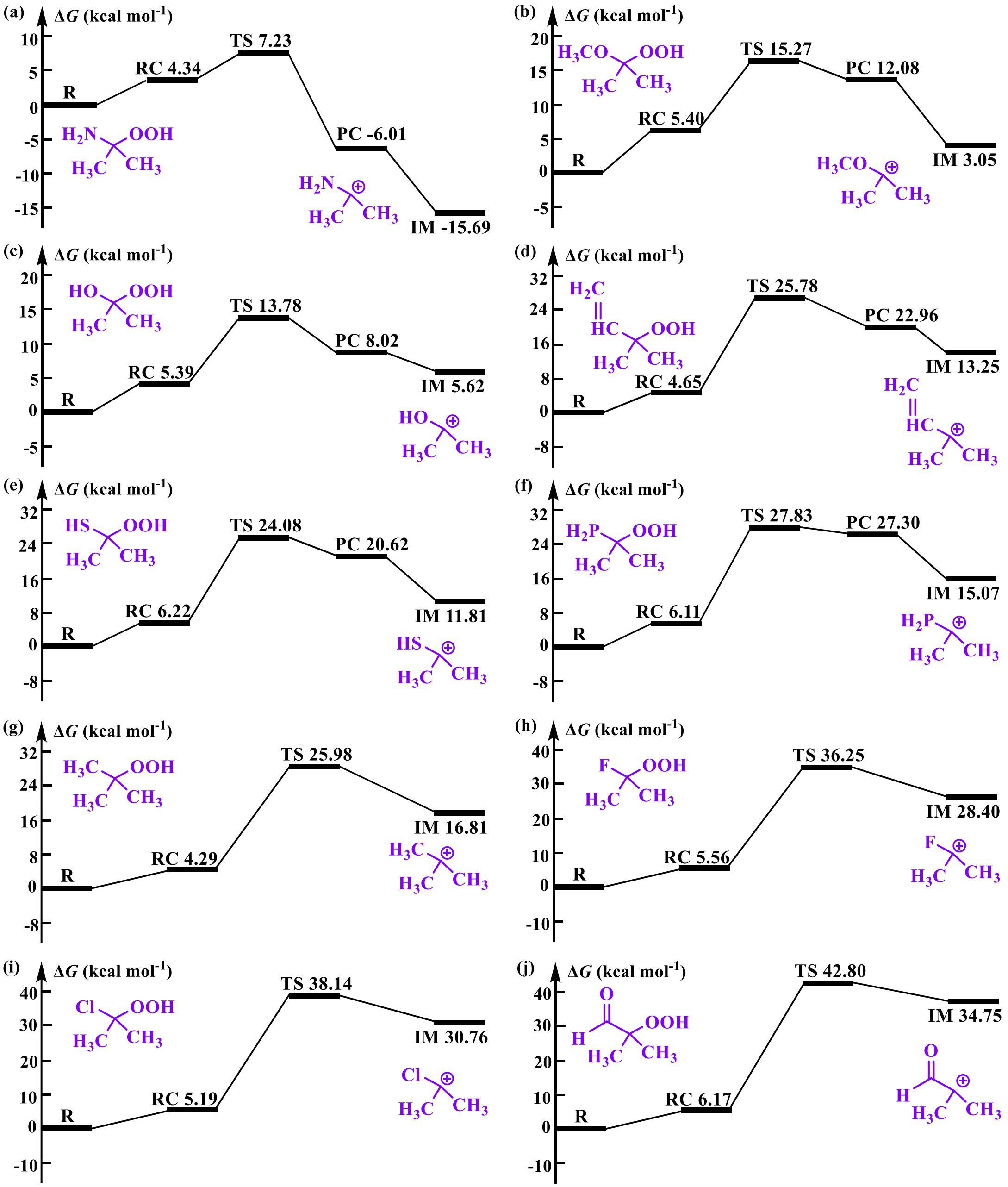

Figure S10. Calculated free-energy surfaces for acid-catalyzed hydrolysis of $C(CH_3)_3OOH$ and ($C(CH_3)_2(X)OOH$) (X = NH_2, OCH_3, OH, CH=CH_2, SH, PH_2, F, Cl and CHO) at the SMD/M06-2X/6-311++G(3df,2pd)//M06-2X/6-31+G(d,p) level. The free energies of ROOH and $H^+(H_2O)_2$ are set to zero (reference state, R). RC, TS, PC and IM represent pre-reactive complexes, transition states, post-reactive complexes and intermediates, respectively.

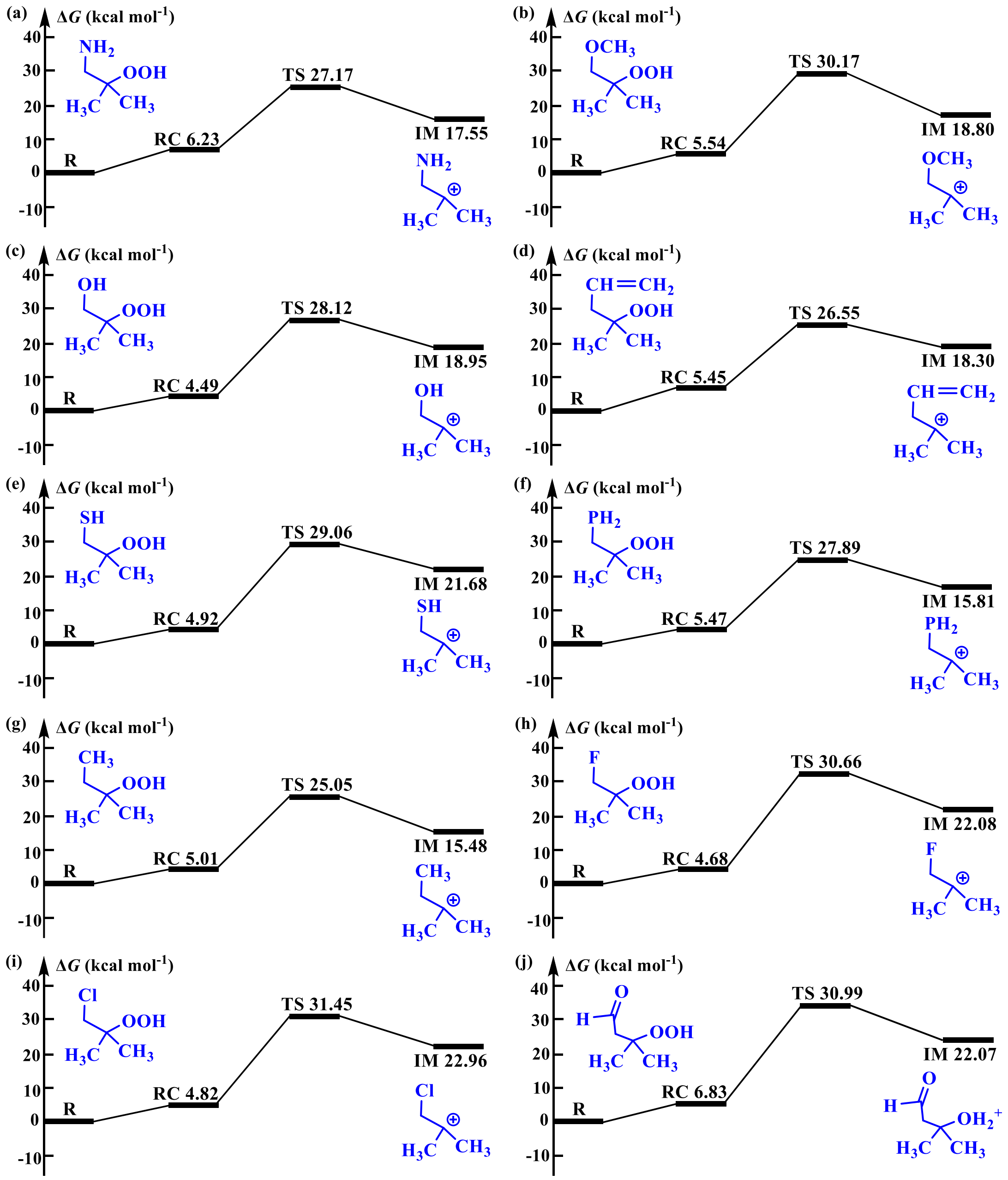

Figure S11. Calculated free-energy surfaces for acid-catalyzed hydrolysis of $C(CH_3)_2(CH_2CH_3)OOH$ and $C(CH_3)_2(CH_2(X))OOH$ (X = NH_2, OCH_3, OH, CH=CH_2, SH, PH_2, F, Cl and CHO) at the SMD/M06-2X/6-311++G(3df,2pd)//M06-2X/6-31+G(d,p) level. The free energies of ROOH and $H^+(H_2O)_2$ are set to zero (reference state, R). RC, TS and IM represent pre-reactive complexes, transition states and intermediates, respectively.

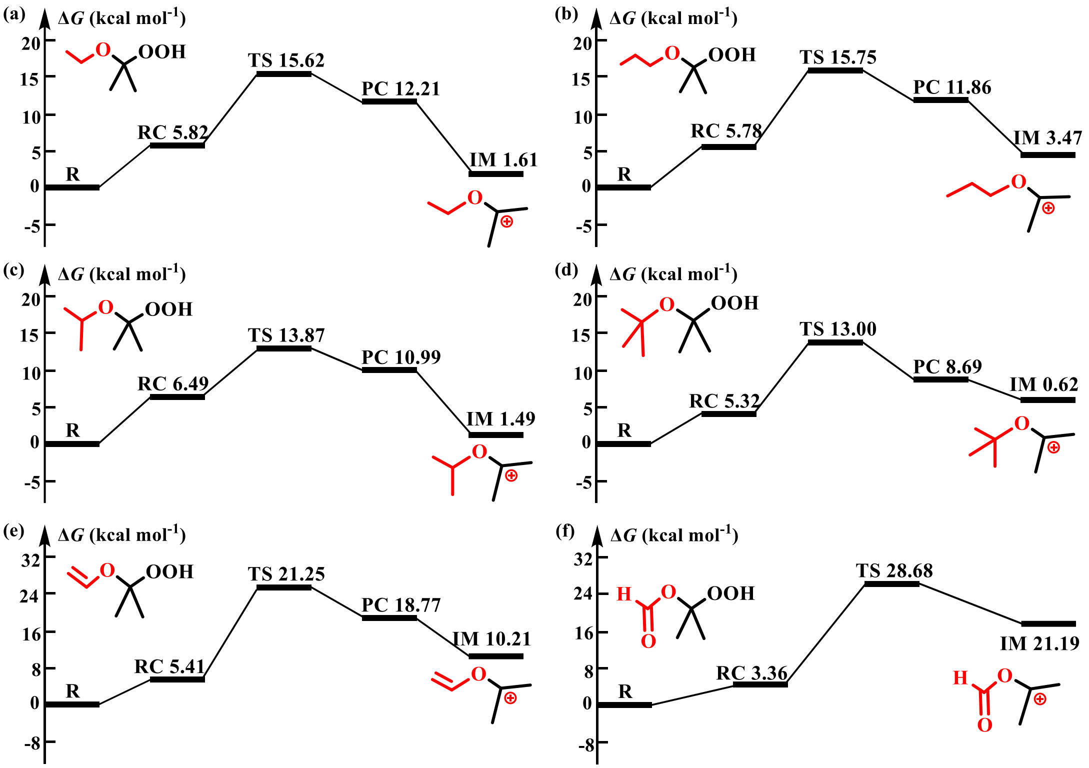

Figure S12. Calculated free-energy surfaces for acid-catalyzed hydrolysis of $C(CH_3)_2(OY)OOH$ (Y = CH_2CH_3, $CH_2CH_2CH_3$, $CH(CH_3)_2$, $C(CH_3)_3$, $CH{=}CH_2$, and CHO) at the SMD/M06-2X/6-311++G(3df,2pd)//M06-2X/6-31+G(d,p) level. The free energies of ROOH and $H^+(H_2O)_2$ are set to zero (reference state, R). RC, TS, PC and IM represent pre-reactive complexes, transition states, post-reactive complexes and intermediates, respectively.

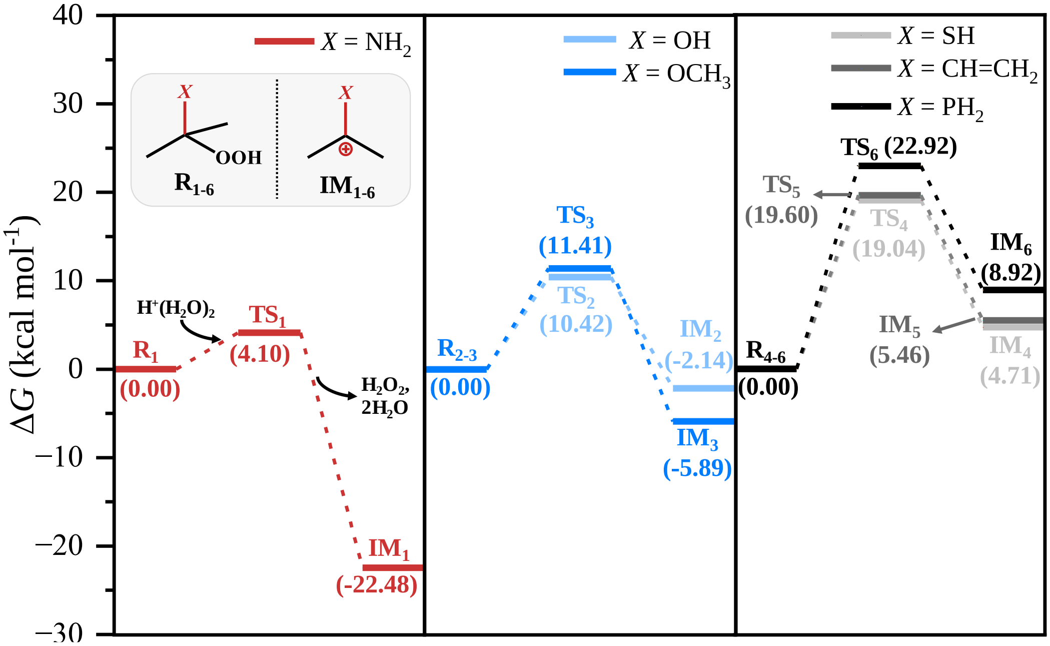

Figure S13. Calculated free-energy surfaces for carbocation formation during the acid-catalyzed hydrolysis of $C(CH_3)_2(X)OOH$, where X = NH_2, OH, OCH_3, $CH=CH_2$, SH, or PH_2. Free energies are computed at ωB97X-D/6-311++G(3df,2pd)//ωB97X-D/6-31+G(d,p) levels with the SMD solvation model, with ROOH and $H^+(H_2O)_2$ set as the reference state at 0 kcal mol^{-1}. Transition states (TS) and intermediates (IM) are labelled.

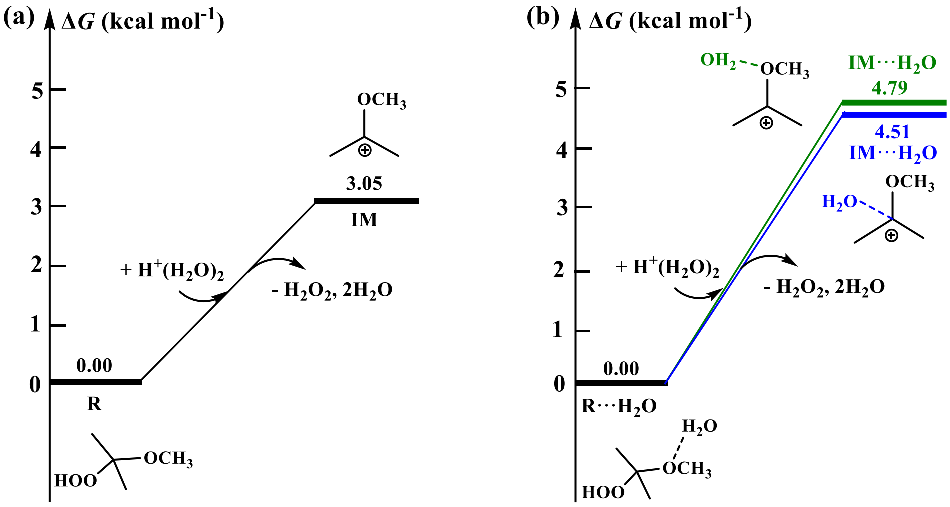

Figure S14. Changes in reaction energetics for carbocation intermediate formation during acid-catalyzed hydrolysis of $C(CH_3)_2(OCH_3)OOH$ under (a) implicit solvation only vs. (b) explicit monohydration. Free energies (*G*) computed at SMD/M06-2X/6-311++G(3df,2pd)//M06-2X/6-31+G(d,p) level. R and IM denote the reactant and carbocation, while $R \cdots H_2O$ and $IM \cdots H_2O$ are their monohydrated forms.

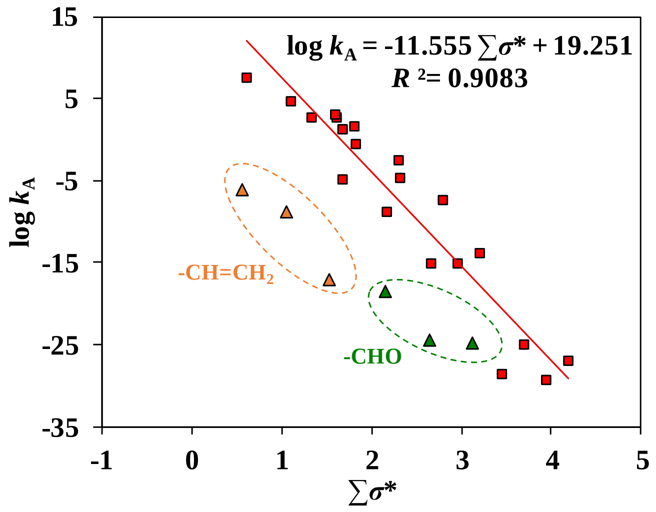

Figure S15. Correlations between the logarithms of the acid-catalyzed hydrolysis second-order rate constants (log k_A) and the sum of Taft constants (∑σ*) of the selected α-substituted ROOH model compounds, including $CH_2(X)OOH$, $CH(CH_3)(X)OOH$, $C(CH_3)_2(X)OOH$, and $C(CH_3)_2(OY)OOH$, where X = $-NH_2$, -OH, $-OCH_3$, $-CH=CH_2$, -SH, $-PH_2$, -F, -Cl, -CHO, and Y = $-CH_2CH_3$, $-CH_2CH_2CH_3$, $-CH(CH_3)_2$, $-C(CH_3)_3$, $-CH=CH_2$, -CHO.

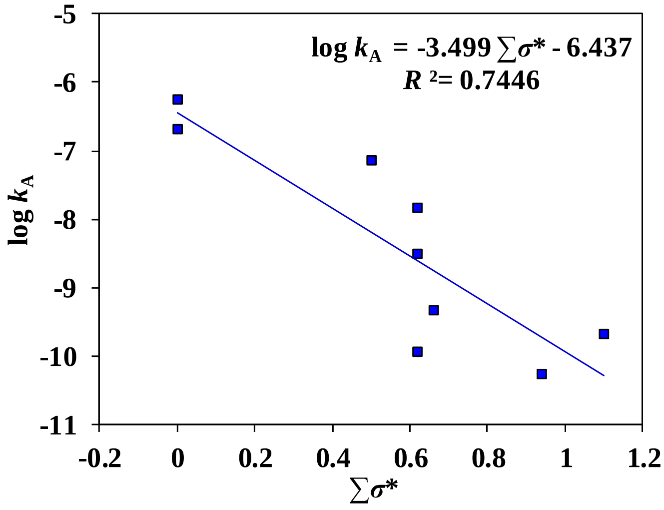

Figure S16. Correlations between the logarithms of the acid-catalyzed hydrolysis second-order rate constants (log k_A) and the sum of Taft constants (∑σ*) for $C(CH_3)_3OOH$ and β-substituted $C(CH_3)_2(CH_2(X))OOH$, where X = $-NH_2$, -OH, $-OCH_3$, $-CH=CH_2$, -SH, $-PH_2$, -F, -Cl, -CHO.

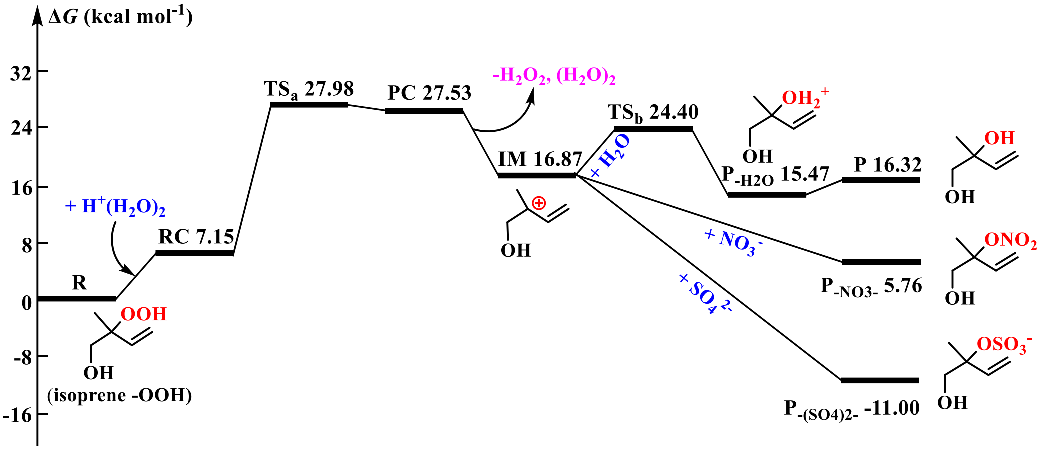

Figure S17. Calculated free-energy surfaces for acid-catalyzed hydrolysis of isoprene-OOH at the SMD/M06-2X/6-311++G(3df,2pd)//M06-2X/6-31+G(d,p) level. The free energies of ROOH and $H^+(H_2O)_2$ are set to zero (reference state). RC, TS_x (x = a, b), PC, IM and P represent pre-reactive complexes, transition states, post-reactive complexes, intermediates and products, respectively.

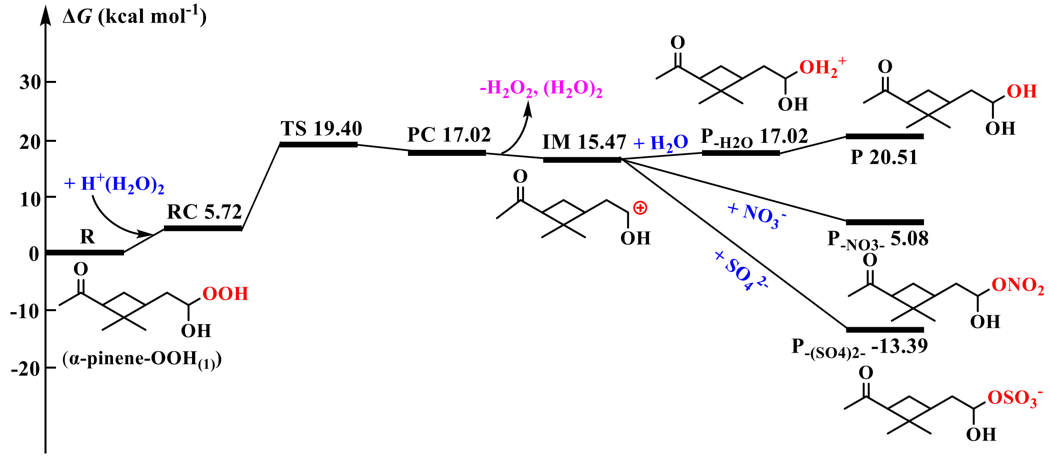

Figure S18. Calculated free-energy surfaces for acid-catalyzed hydrolysis of α-pinene-OOH$_{(1)}$ at the SMD/M06-2X/6-311++G(3df,2pd)//M06-2X/6-31+G(d,p) level. The free energies of ROOH and $H^+(H_2O)_2$ are set to zero (reference state). RC, TS, PC, IM and P represent pre-reactive complexes, transition states, post-reactive complexes, intermediates and products, respectively.

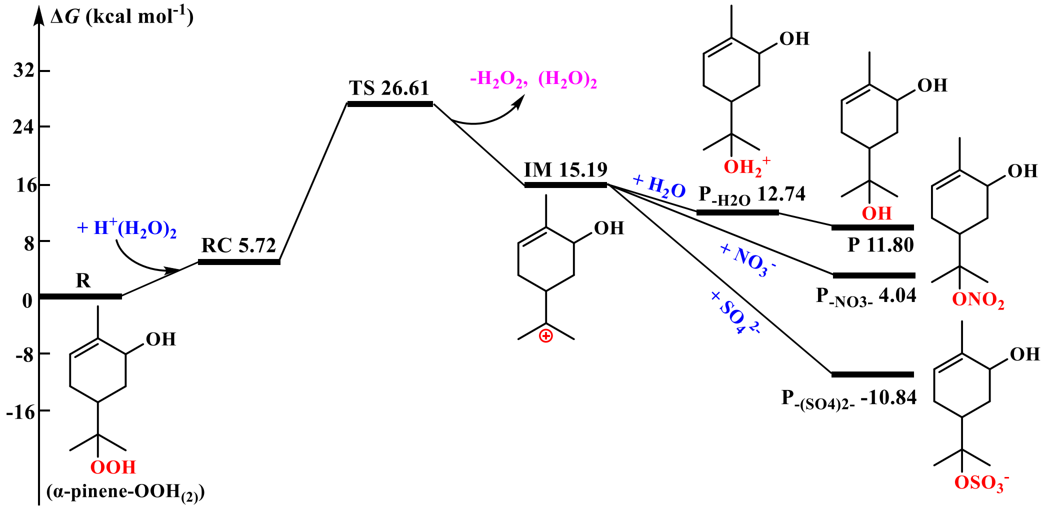

Figure S19. Calculated free-energy surfaces for acid-catalyzed hydrolysis of α-pinene-OOH$_{(2)}$ at the SMD/M06-2X/6-311++G(3df,2pd)//M06-2X/6-31+G(d,p) level. The free energies of ROOH and $H^+(H_2O)_2$ are set to zero (reference state). RC, TS, IM and P represent pre-reactive complexes, transition states, intermediates and products, respectively.

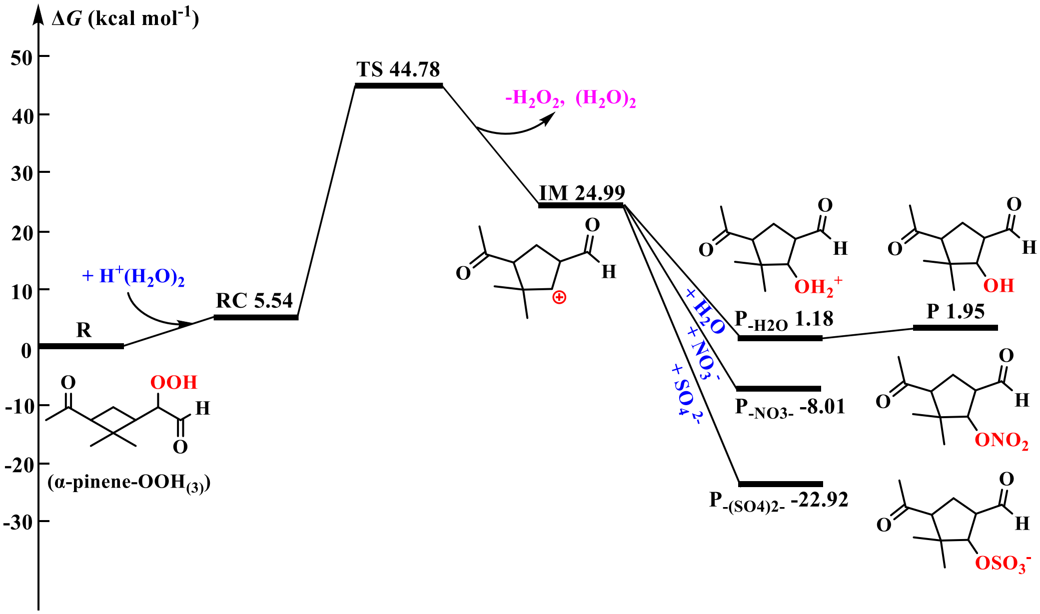

Figure S20. Calculated free-energy surfaces for acid-catalyzed hydrolysis of α-pinene-OOH$_{(3)}$ at the SMD/M06-2X/6-311++G(3df,2pd)//M06-2X/6-31+G(d,p) level. The free energies of ROOH and $H^+(H_2O)_2$ are set to zero (reference state). RC, TS, IM and P represent pre-reactive complexes, transition states, intermediates and products, respectively.

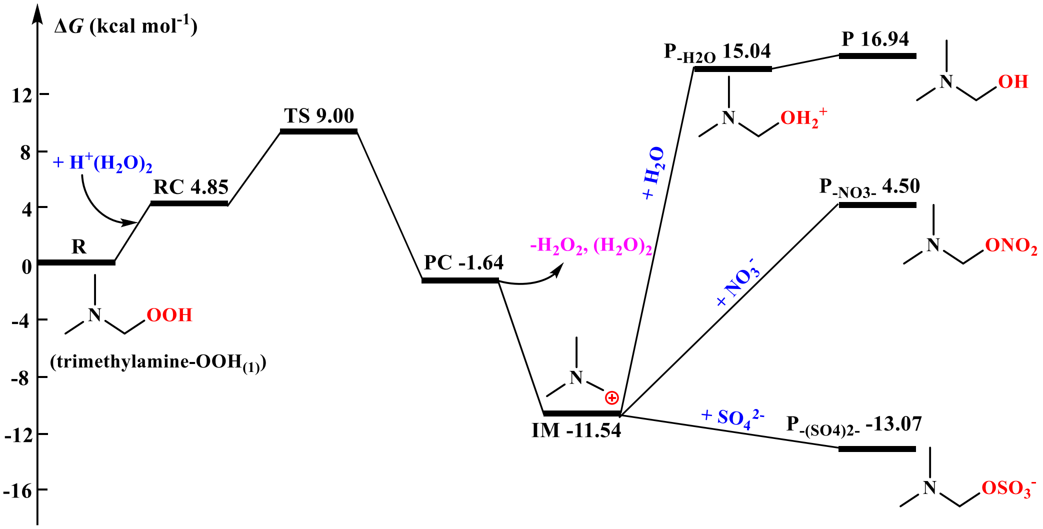

Figure S21. Calculated free-energy surfaces for acid-catalyzed hydrolysis of trimethylamine-OOH$_{(1)}$ at the SMD/M06-2X/6-311++G(3df,2pd)//M06-2X/6-31+G(d,p) level. The free energies of ROOH and $H^+(H_2O)_2$ are set to zero (reference state). RC, TS, PC, IM and P represent pre-reactive complexes, transition states, post-reactive complexes, intermediates and products, respectively.

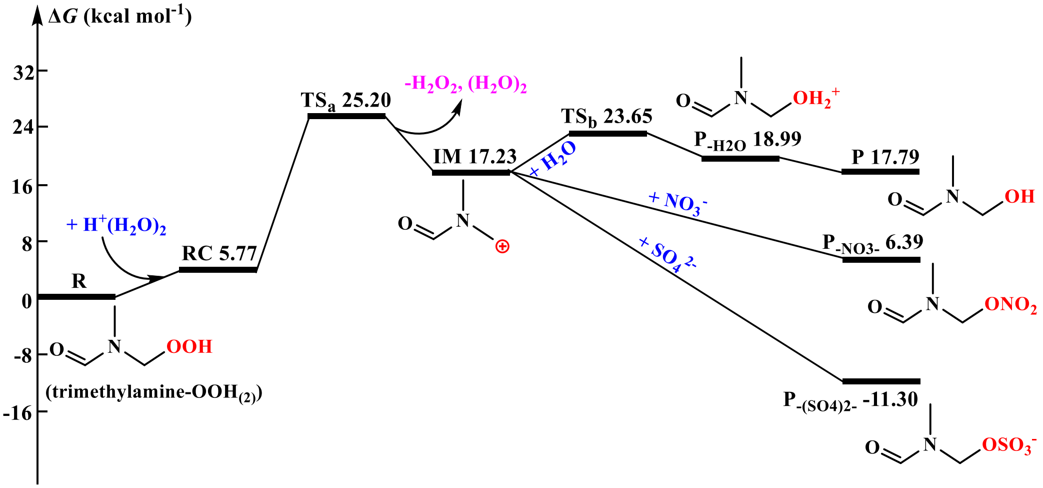

Figure S22. Calculated free-energy surfaces for acid-catalyzed hydrolysis of trimethylamine-OOH$_{(2)}$ at the SMD/M06-2X/6-311++G(3df,2pd)//M06-2X/6-31+G(d,p) level. The free energies of ROOH and $H^+(H_2O)_2$ are set to zero (reference state). RC, TS$_x$ (x = a, b), IM and P represent pre-reactive complexes, transition states, intermediates and products, respectively.

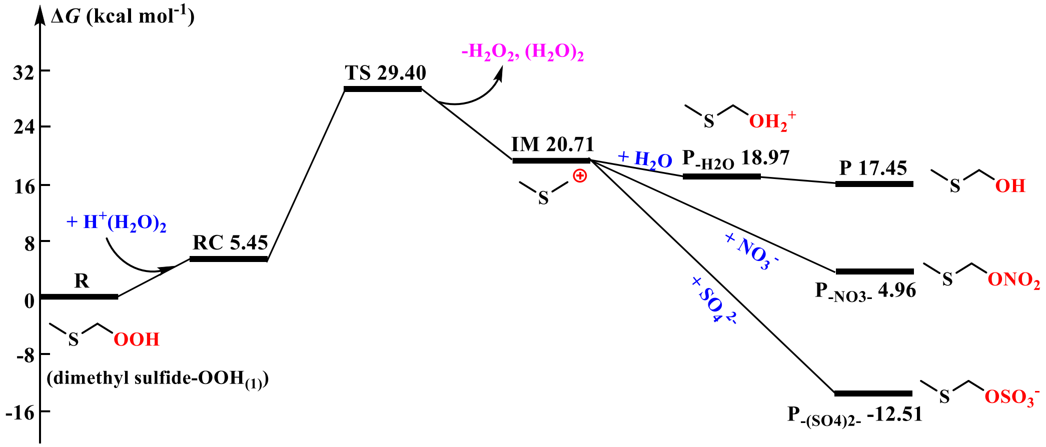

Figure S23. Calculated free-energy surfaces for acid-catalyzed hydrolysis of dimethyl sulfide-OOH$_{(1)}$ at the SMD/M06-2X/6-311++G(3df,2pd)//M06-2X/6-31+G(d,p) level. The free energies of ROOH and $H^+(H_2O)_2$ are set to zero (reference state). RC, TS, IM and P represent pre-reactive complexes, transition states, intermediates and products, respectively.

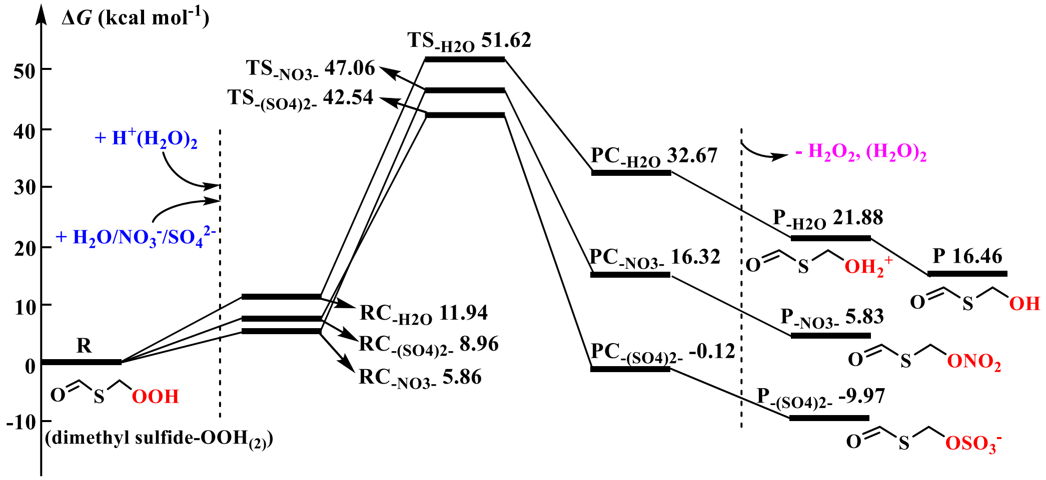

Figure S24. Calculated free-energy surfaces for acid-catalyzed hydrolysis of dimethyl sulfide-OOH$_{(2)}$ at the SMD/M06-2X/6-311++G(3df,2pd)//M06-2X/6-31+G(d,p) level. The free energies of ROOH, $H^+(H_2O)_2$, and $H_2O/NO_3^-/SO_4^{2-}$ are set to zero (reference state). RC, TS, PC and P represent pre-reactive complexes, transition states, post-reactive complexes and products, respectively.

Table S1. Taft (σ^*) constants of different substituents (Perrin et al., 1981).

Substituents	σ^*	**Substituents**	σ^*
-H	0.49	$-CH_3$	0.00
$-NH_2$	0.62	$-CH_2NH_2$	0.50
$-N(CH_3)_2$	0.32	$-CH_2OH$	0.62
-OH	1.34	$-CH_2OCH_3$	0.66
$-OCH_3$	1.81	$-CH_2SH$	0.62
$-OCH_2CH_3$	1.68	$-CH_2PH_2$	—
$-OCH_2CH_2CH_3$	1.68	$-CH_2CH=CH_2$	0.00
$-OCH(CH_3)_2$	1.62	$-CH_2F$	1.10
$-OC(CH_3)_3$	—	$-CH_2Cl$	0.94
$-OCH=CH_2$	—	$-CH_2CHO$	0.62
-OCHO	—		
-SH	1.68		
$-SCH_3$	1.56		
$-PH_2$	—		
$-CH=CH_2$	0.56		
-F	3.21		
-Cl	2.96		
-CHO	2.15		

Table S2. Sum of Taft σ^* constants ($\sum\sigma^*$) of the selected 45 ROOHs model compounds.

Model compounds	***X*/*Y***	$\sum\boldsymbol{\sigma}^*$	**Model compounds**	***X*/*Y***	$\sum\boldsymbol{\sigma}^*$
CH_3CH_2OOH	—	0.00	$CH(CH_3)_2OOH$	—	0.49
$C(CH_3)_3OOH$	—	0.98			
$CH_2(X)OOH$	NH_2	1.60	$CH(CH_3)(X)OOH$	NH_2	1.11
	OH	2.32		OH	1.83
	OCH_3	2.79		OCH_3	2.30
	SH	2.66		SH	2.17
	$CH{=}CH_2$	1.54		$CH{=}CH_2$	1.05
	PH_2	—		PH_2	—
	F	4.19		F	3.70
	Cl	3.94		Cl	3.45
	CHO	3.13		CHO	2.64
$C(CH_3)_2(X)OOH$	NH_2	0.62	$C(CH_3)_2(CH_2(X))OOH$	NH_2	0.50
	OH	1.34		OH	0.62
	OCH_3	1.81		OCH_3	0.66
	SH	1.68		SH	0.62
	$CH{=}CH_2$	0.56		$CH{=}CH_2$	0.00
	PH_2	—		PH_2	—
	F	3.21		F	1.10
	Cl	2.96		Cl	0.94
	CHO	2.15		CHO	0.62
$C(CH_3)_2(O(Y))OOH$	CH_2CH_3	1.68			
	$CH_2CH_3CH_3$	1.68			
	$CH(CH_3)_2$	1.62			
	$C(CH_3)_3$	—			
	$CH{=}CH_2$	—			
	CHO	—			

Table S3. Calculated acid-catalyzed hydrolysis second-order rate constants (k_A) and the corresponding lifetimes ($\tau_{1/e}$) of selected 45 ROOHs model compounds under two selected scenarios (Inland regions, China (pH 3.8) and Southeastern United States (pH 0.9)).

Model compounds	***X*/*Y***	**k_A (L mol^{-1} s^{-1})**	**$\tau_{1/e,\ pH\ 3.8}$**	**$\tau_{1/e,\ pH\ 0.9}$**
CH_3CH_2OOH	—	1.58×10^{-21}	4.6×10^{19} d	5.8×10^{16} d
$CH(CH_3)_2OOH$	—	1.12×10^{-14}	6.5×10^{12} d	8.2×10^{9} d
$C(CH_3)_3OOH$	—	5.50×10^{-7}	1.3×10^{5} d	1.7×10^{2} d
$CH_2(X)OOH$	NH_2	1.01×10^{3}	6.3 s	< 1 s
	OH	1.94×10^{-5}	3.8×10^{3} d	4.7 d
	OCH_3	4.45×10^{-8}	1.6×10^{6} d	2.1×10^{3} d
	SH	6.77×10^{-16}	1.1×10^{14} d	1.4×10^{11} d
	$CH=CH_2$	8.11×10^{-18}	9.0×10^{15} d	1.1×10^{13} d
	PH_2	2.08×10^{-16}	3.5×10^{14} d	4.4×10^{11} d
	F	1.07×10^{-27}	—	—
	Cl	4.63×10^{-30}	—	—
	CHO	1.43×10^{-25}	—	—
$CH(CH_3)(X)OOH$	NH_2	5.60×10^{4}	< 1 s	< 1 s
	OH	3.20×10^{-1}	5.5 h	24.8 s
	OCH_3	3.24×10^{-3}	22.6 d	40.9 min
	SH	1.40×10^{-9}	5.2×10^{7} d	6.6×10^{4} d
	$CH=CH_2$	1.62×10^{-9}	4.5×10^{7} d	5.7×10^{4} d
	PH_2	2.73×10^{-14}	2.7×10^{12} d	3.4×10^{9} d
	F	1.05×10^{-25}	—	—
	Cl	2.88×10^{-29}	—	—
	CHO	3.73×10^{-25}	—	—
$C(CH_3)_2(X)OOH$	NH_2	3.10×10^{7}	< 1 s	< 1 s
	OH	4.87×10^{2}	13.0 s	< 1 s
	OCH_3	3.93×10^{1}	2.7 min	< 1 s
	SH	1.36×10^{-5}	5.4×10^{3} d	6.8 d
	$CH=CH_2$	7.72×10^{-7}	9.5×10^{4} d	1.2×10^{2} d
	PH_2	2.42×10^{-8}	3.0×10^{6} d	3.8×10^{3} d
	F	1.62×10^{-14}	—	—
	Cl	6.65×10^{-16}	—	—
	CHO	2.54×10^{-19}	—	—

$C(CH_3)_2(CH_2(X))OOH$	NH_2	7.38×10^{-8}	—	—
	OH	1.49×10^{-8}	—	—
	OCH_3	4.66×10^{-10}	—	—
	SH	3.03×10^{-9}	—	—
	$CH{=}CH_2$	2.11×10^{-7}	—	—
	PH_2	2.19×10^{-8}	—	—
	F	2.04×10^{-10}	—	—
	Cl	5.36×10^{-11}	—	—
	CHO	1.17×10^{-10}	—	—
$C(CH_3)_2(O(Y))OOH$	CH_2CH_3	2.17×10^{1}	4.9 min	< 1 s
	$CH_2CH_3CH_3$	1.76×10^{1}	6.0 min	< 1 s
	$CH(CH_3)_2$	4.16×10^{2}	15.2 s	< 1 s
	$C(CH_3)_3$	1.81×10^{3}	3.5 s	< 1 s
	$CH{=}CH_2$	1.62×10^{-3}	45.1 d	1.4 h
	CHO	5.80×10^{-9}	1.3×10^{7} d	1.6×10^{4} d

Table S4. Calculated acid-catalyzed hydrolysis second-order rate constants (k_A) and the corresponding lifetimes ($\tau_{1/e}$) of 8 atmospheric ROOHs under two selected scenarios (Inland regions, China (pH 3.8) and Southeastern United States (pH 0.9)).

Compounds Name	**k_A (L mol^{-1} s^{-1})**	**$\tau_{1/e,\ pH\ 3.8}$**	**$\tau_{1/e,\ pH\ 0.9}$**
trimethylamine-OOH$_{(1)}$	1.56×10^{6}	< 1 s	< 1 s
α-pinene-OOH$_{(1)}$	3.68×10^{-2}	2 d	3.6 min
trimethylamine-OOH$_{(2)}$	2.05×10^{-6}	3.6×10^{4} d	45 d
α-pinene-OOH$_{(2)}$	1.90×10^{-7}	3.8×10^{5} d	484 d
isoprene-OOH	1.88×10^{-8}	3.9×10^{6} d	4.9×10^{3} d
dimethyl sulfide-OOH$_{(1)}$	1.71×10^{-9}	4.3×10^{7} d	5.4×10^{4} d
α-pinene-OOH$_{(3)}$	8.99×10^{-21}	8.1×10^{18} d	1.0×10^{16} d
dimethyl sulfide-OOH$_{(2)}$	8.66×10^{-26}	8.4×10^{23} d	1.0×10^{21} d

References

Enami, S.: Proton-catalyzed decomposition of multifunctionalized organic hydroperoxides derived from the reactions of criegee intermediates with ethylene glycol in aqueous organic media, ACS Earth Space Chem., 6, 1937-1947, 10.1021/acsearthspacechem.2c00142, 2022.

Hu, M., Chen, K., Qiu, J., Lin, Y., Tonokura, K., and Enami, S.: Decomposition mechanism of α-alkoxyalkyl-hydroperoxides in the liquid phase: temperature dependent kinetics and theoretical calculations, Environ Sci Atmos, 2, 241-251, 10.1039/d1ea00076d, 2022.

Perrin, D. D., Dempsey, B., and Serjeant, E. P.: p*K*a prediction for organic acids and bases, Champman and Hall: New York, 1981.

Qiu, J., Tonokura, K., and Enami, S.: Proton-catalyzed decomposition of α-hydroxyalkyl-hydroperoxides in water, Environ. Sci. Technol., 54, 10561-10569, 10.1021/acs.est.0c03438, 2020.